arXiv:1606.09417v1 [astro-ph.IM] 30 Jun 2016

First measurement of polarisation asymmetry of a gamma-ray beam between 1.74 to 74 MeV with the HARPO TPC

P. Gros*[1], S. Amano[2], D. Attié[3], D. Bernard[1], P. Bruel[1], D. Calvet[3], P. Colas[3], S. Daté[4], A. Delbart[3], M. Frotin[1], Y. Geerebaert[1], B. Giebels[1], D. Götz[5], S. Hashimoto[2], D. Horan[1], T. Kotaka[2], M. Louzir[1], Y. Minamiyama[2], S. Miyamoto[2], H. Ohkuma[4], P. Poilleux[1], I. Semeniouk[1], P. Sizun[3], A. Takemoto[2], M. Yamaguchi[2], and S. Wang[1]

[1]LLR, École Polytechnique, CNRS/IN2P3, Palaiseau, France
[2]LASTI, University of Hyôgo, Japan
[3]Irfu, CEA-Saclay, France
[4]JASRI/SPring8, Japan
[5]AIM, CEA/DSM-CNRS-Université Paris Diderot, France

July 1, 2016

Abstract

Current γ-ray telescopes suffer from a gap in sensitivity in the energy range between 100 keV and 100 MeV, and no polarisation measurement has ever been done on cosmic sources above 1 MeV. Past and present e^+e^- pair telescopes are limited at lower energies by the multiple scattering of electrons in passive tungsten converter plates. This results in low angular resolution, and, consequently, a drop in sensitivity to point sources below 1 GeV. The polarisation information, which is carried by the azimuthal angle of the conversion plane, is lost for the same reasons.

HARPO (Hermetic ARgon POlarimeter) is an R&D program to characterise the operation of a gaseous detector (a Time Projection Chamber or TPC) as a high angular-resolution and sensitivity telescope and polarimeter for γ rays from cosmic sources. It represents a first step towards a future space instrument in the MeV-GeV range.

We built and characterised a 30cm cubic demonstrator [SPIE 91441M], and put it in a polarised γ-ray beam at the NewSUBARU accelerator in Japan. Data were taken at photon energies from 1.74 MeV to 74 MeV and with different polarisation configurations.

We describe the experimental setup in beam. We then describe the software we developed to reconstruct the photon conversion events, with special focus on low energies. We also describe the thorough simulation of the detector used to compare results. Finally we will present the performance of the detector as extracted from this analysis and preliminary measurements of the polarisation asymmetry.

This beam-test qualification of a gas TPC prototype in a γ-ray beam could open the way to high-performance γ-ray astronomy and polarimetry in the MeV-GeV energy range in the near future.

*corresp. author: philippe.gros@llr.in2p3.fr

1 Introduction

γ rays are produced in some of the most violent objects in the Universe, such as pulsars, active galactic nuclei (AGN) and γ-ray bursts (GRBs). The field of γ-ray astronomy is concerned with the study of these non-thermal emissions, thus allowing us to gain an understanding of the detailed nature of these extreme objects.

Below $\approx$1 MeV Compton telescopes ($\gamma e^- \to \gamma e^-$) are highly performant, but the Compton cross-section, and therefore the telescopes sensitivity, decreases with photon energy. Above $\approx$1 GeV pair telescopes ($\gamma Z \to Ze^+e^-$) are highly performant, but they use high-Z converter plates (tungsten in Fermi's Large Area Telescope, *Fermi*-LAT) which severely degrade their resolution at low energy. The gap in resolution and sensitivity in the MeV-GeV range hinders the study of many broad-band astrophysical emitters. This includes for instance blazars, which are postulated to comprise a sequence, the so-called blazar sequence [], whose properties could be biased by the absence of sensitive observations in the MeV-GeV range. It is also difficult to distinguish sources in crowded regions of the sky, such at the galactic plane. To a large extent, the MeV-GeV sensitivity gap [1] is an angular resolution issue. The angular resolution of pair telescopes can be improved, from the *Fermi*-LAT's $\approx 5^\circ$ at 100 MeV [2] to $1-2^\circ$, by the use of pure silicon trackers, i.e. without any tungsten converter plates [3–5].

An even better resolution of $\approx 0.4^\circ$ can, however, be obtained with a gaseous detector such as a time-projection chamber (TPC). Together with the development of high-performance Compton telescope, filling the sensitivity gap for point-like sources at a level of $\approx 10^{-6}$ MeV/(cm^{2}s) is within reach (see Ref. [6] and Fig. 1).

Furthermore, the use of a low density converter-tracker, such as a gaseous detector, enables the measurement of the polarisation fraction before multiple scattering ruins the azimuthal information carried by the pair [7]. Since the sensitivity of the Compton process to polarisation decreases as $1/E_\gamma$ [7], this is the only possibility for high-energy polarimetry. The polarisation of sources was never available for γ-rays above 1 MeV for reasons explained in Ref. [8]. At lower energies, in the radio to X-ray energy range, the measurement of the linear polarisation of the emission is a powerful tool for understanding the characteristics of cosmic sources. It gives us access to information on the magnetic-field structure not otherwise readily available. Extending the measurement to γ rays will open new levels of understanding of these sources.

γ-ray polarimetry would, for example, provide insight into the understanding of the value and turbulence of magnetic fields in the γ-ray emitting jet structures of most γ-ray emitting sources. It could enable us to distinguish between the leptonic and hadronic nature of the emitting particles in blazars [9], a long-standing open question in AGN research.

2 The HARPO Experimental setup

The HARPO (Hermetic ARgon POlarimeter) detector is a demonstrator of the performance of a TPC for measuring polarised γ rays. It was designed for a validation on the ground, in a photon beam. The most critical constraints related to potential space operation were taken into account, such as the reduced number of electronic channels, and long-term gas quality preservation.

2.1 The HARPO TPC

The HARPO detector [10] is a 30 cm cubic TPC, filled with Ar:isobutane (95:5) gas mixture up to 5 bar. It is equipped with a drift cage providing a 220 V/cm drift field. The electrons produced by ionisation of the gas drift along the electric field toward the readout plane at

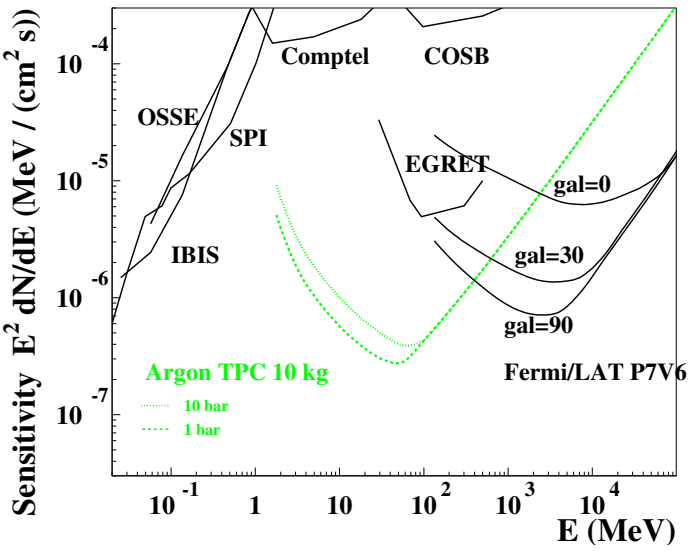

Figure 1: Differential sensitivity as a function of energy (argon-gas-based HARPO TPC, green) compared to the 90° galactic latitude performance of the *Fermi*-LAT [2] and of the Compton telescope COMPTEL [1]. Adapted from [6].

a constant velocity $v_{drift} \approx 3.3\,\mathrm{cm}/\mu\mathrm{s}$. The arrival time can therefore be converted to the Z-coordinate with the formula:

$$Z = v_{drift}(t_{signal} - t_0) \tag{1}$$

The readout plane is equipped with two Gas Electron Multipliers (GEMs) and one Micromesh Gas Structure (Micromegas) to amplify the electrons. The amplified electrons' signal is collected by two sets of perpendicular strips (regular strips in the X-direction, and pads connected together by an underlying strip in the Y-direction, see Fig. 2). The signals from the strips are read out and digitised with a set of AFTER chips [11] and associate Front End Cards (FECs).

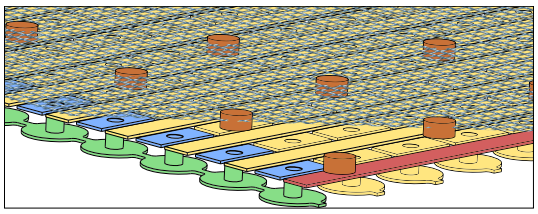

Figure 2: Detail of the micromegas and readout strips configuration.

The signal recorded for an event in the TPC comprises the XZ and YZ projections of the deposited charge in the gas, where the Z direction corresponds to the drift time of the electrons. Several examples of pair-conversion events in the TPC are shown in Fig. 3.

2.2 Data taking at the NewSUBARU gamma-ray beam line

The HARPO TPC was set up in the NewSUBARU polarised photon beam line [12]. The photon beam is produced by Inverse Compton Scattering (ICS) of an optical laser on a high

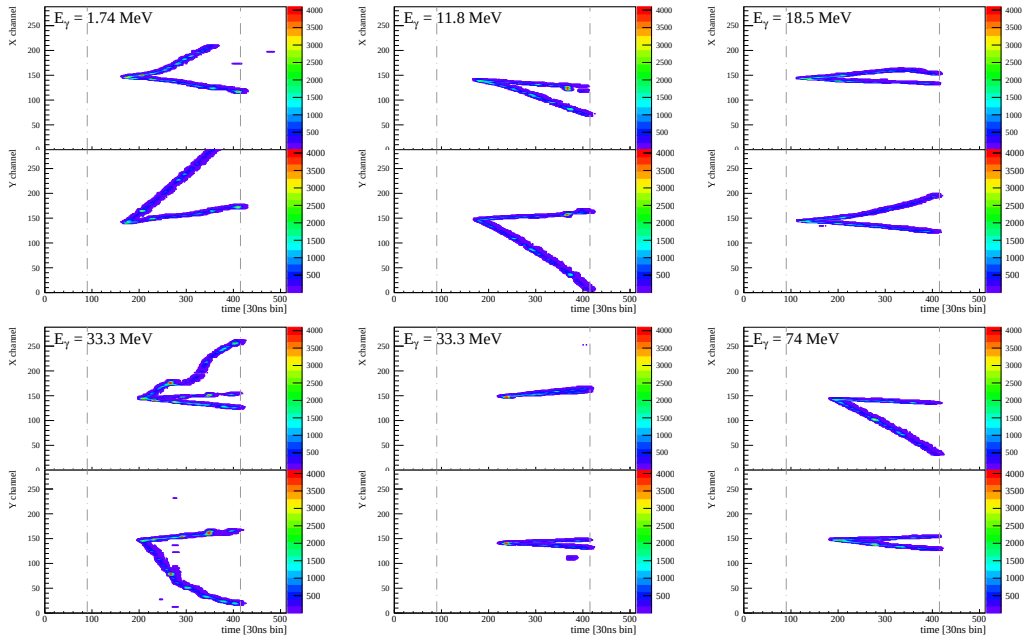

Figure 3: Typical conversion events in the HARPO detector, for different photon energies. The top and bottom parts of the images show the two projections XZ and YZ (where Z is proportional to the drift time of the electrons in the TPC). We can see that at higher energies, there is less scattering, and smaller opening angles. On the top left we see an asymmetry in the track directions, although the photon beam is in the Z direction. This is because part of the momentum is taken by the undetected recoiling nucleus. In the bottom left, we see a triplet conversion. In the bottom middle, we see that in the top projection (XZ) the two tracks are overlapping.

energy (0.6-1.5 GeV) electron beam. Using lasers of various wavelengths and different beam energies (as described in more detail in [13]), we scanned 13 photon energies from 1.74 MeV to 74 MeV.

In order to minimise systematic effects due to the geometry of the detector, the detector itself was rotated around the beam axis to 4 different angular positions (-45, 0, 45 and 90 °). Finally, for some configurations (in particular at low energy), data were also taken with randomly polarised photons.

Most data were taken at a TPC pressure of 2.1 bar. A short scan of pressure up to 4.0 bar was also done in the beam.

2.3 Electronics saturation

After analysis we found that the charge preamplifiers of the AFTER chips were often saturated during the data taking in beam. If too much charge was accumulated on a single channel (which was the case in particular when a track was aligned with the drift direction), the preamplifier stopped responding linearly, and quickly stopped giving any signal at all. The effects on our data were amplified by the beam configuration, which accumulated the signal on a few channels. They were also made worse by the high luminosity. This was reduced by changing the detector alignment, but it still affects a large fraction of the beam data. Fortunately, most of the pair conversion information is contained in the early part of the event, before the saturation. The reconstruction was therefore adapted to minimise the

effect on the final results.

This saturation can be greatly and easily reduced by changing the dynamic range in the programmable electronics. This should not affect the performance of the detector because the charge resolution is not critical for the reconstruction. This was unfortunately not known at the time of the data taking in beam. This effect will have very little impact on the performance for measuring cosmic photons that have random directions and a lower rate.

3 Simulation of the HARPO detector

We developed a complete simulation to describe the response of the HARPO detector. It contains three main components: an event generator describing the conversion of photons in the gas, a Geant4 based simulation of the interaction of the electron-positron pair with the gas, and a custom description of the processes and geometry of the TPC.

3.1 Photon conversion event generator

There was no event generator available for photon conversion to e^+e^- pair [14–17] that fulfils the following requirements:

- exact down to threshold, that is, without any low-energy approximations;
- complete, that is, that provides a sampling of the five-dimensional differential cross section;
- polarised.

We therefore developed such a tool and characterised it with respect to expressions for 1D projection calculations published in the past (section 3 of Ref. [7]).

3.2 Electron propagation and ionisation with Geant4

The position and momentum of the electron and positron are used as input for a simple simulation using Geant4 [16]. Only the gas volume of the TPC is described in this simulation. The electrons are propagated through the gas, taking into account, in particular, multiple scattering and gas ionisation. This simulation provides the position of ionisation interactions in the gas volume, as well as the number of ionisation electrons.

3.3 TPC response

Since Geant4 cannot describe the electron drift and electronics response, we developed a standalone simulation of the HARPO TPC based on work done for the ALICE TPC [18] and LCTPC [19]. This simulation takes as input a list of the ionisation electrons with their position (provided by Geant4). For each individual electron, it applies a drift through the gas, taking into account drift velocity, Gaussian diffusion, and potential capture. All the parameters are calibrated from the data, and are found to be consistent with values obtained using simulations with Magboltz [20].

The amplification and readout of the electrons is described with a simple exponential gain fluctuation and Gaussian spatial spread. The actual detector geometry is used to segment the signal. The gain and space response are also calibrated using experimental data.

Finally, the electronics time response including shaping, noise and digitisation is added. The saturation effects mentioned above, which noticeably affected our data, are also implemented.

The simulation output is in the same format as the real data, and all the reconstruction and analysis are applied identically to both.

4 Reconstruction of photon conversions into e^+e^- pairs in HARPO

The diffusion of the signal, together with the large scattering of the particles in the gas, make it very difficult to use conventional tracking methods. The large multiple scattering prevents the use of straight line finding algorithms such as Hough transforms [21]. On the other hand, the spread of the electron signal (due to diffusion and electronics shaping) makes it difficult to reconstruct the original cluster position. The large systematic bias in the clustering prevents the use of a Kalman filter [22] to take into account multiple scattering. Our approach was therefore to focus on the specific geometry that we are looking for: pair vertices. We developed an original method to efficiently find vertices, and determine the direction of the two associated particles. Subsequently, vertices of the two projections, XZ and YZ, are associated with each other to recover the full 3D description of the vertex. The method does not yet include a filter to exclude fake vertices.

4.1 2D Vertex finding

We are looking for the point of conversion of a photon into a e^+e^- pair. This means the starting point of two tracks, with an angle strictly inferior to π.

We scan all the positions containing signal in a grid of 5 channels$\times$10 time bins (which corresponds to the typical spread of the electron signal). We then trace an ellipse around each point and measure the longest arc which does not cross any region containing signal. If this arc is longer than half the circle, it is identified as a vertex (see Fig. 4). The radius of the ellipse should be larger than the width of the signal (i.e. the electron diffusion and electronics time response), but small enough to avoid being affected by other tracks. They are taken to be about twice the typical width of the signal. This procedure relies on the very low noise in the data.

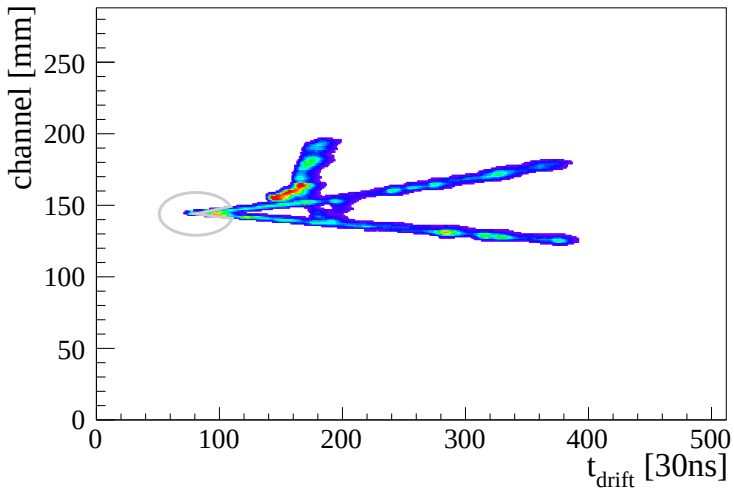

Figure 4: Vertex finding procedure on a pair conversion event with a δ-electron. Circles are drawn around signal regions. If the longest arc without signal is larger than half an ellipse, the region is considered as a vertex candidate.

Once a region of interest is found, the position of the vertex is estimated as the centre of gravity of all of the signal within that region.

This method also selects the ends of single tracks and some other regions. It is necessary, therefore to apply further criteria to select real photon conversion regions. In the case of the beam data, proximity to the beam position is a sufficient criterion, but for a more generic use, a better description of the event will be needed.

4.2 2D Vertex fitting

Once a vertex candidate has been found, we can map the signal around it in polar coordinates (Fig. 5, left). We only keep the regions with a continuous signal from the vertex (Fig. 5, middle).

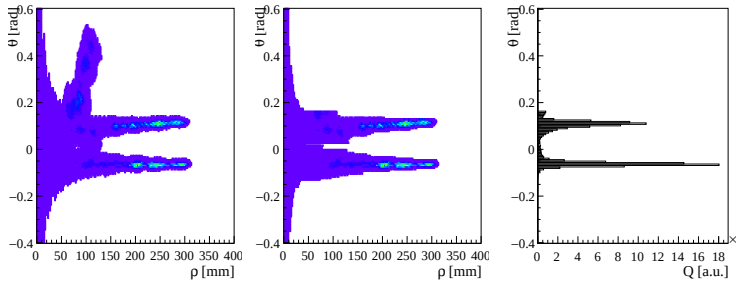

Figure 5: Vertex fitting procedure. Left: polar distribution of charge around the vertex candidate. Middle: only regions with nearly continuous signal from the vertex ($\rho = 0$) are kept (gaps of one bin are allowed). This reduces the effect of scattering and background. Most of the signal from the δ-electron is removed. Right: angular distribution with two clear peaks corresponding to the two associated tracks. A peak search on the distribution defines the direction of the pair of particles.

From this, we project the charge distribution as a function of the polar angle around the vertex candidate (Fig. 5, right). The peaks of the distribution indicate the direction of the tracks originating from the vertex.

4.3 Combining 2D vertices for 3D configuration

Finally, we associate each XZ projection of a vertex with its YZ projection, and correctly associate the two tracks associated with each vertex, so that we recover a full 3D description of the e^+e^- pair. This is done by comparing the charge profiles of the tracks as a function of the Z-coordinate (drift time). This procedure, called "matching" is described in Fig. 6.

For each 2D vertex, we associate with each of the 2 tracks the signal contained in a region around the track direction. From this signal, we create the charge profile as a function of Z (or the drift time). The electron diffusion in the drift volume, and between the GEM plates, create a strong signal correlation at short distances (smaller than $\sim$ 1mm). We know therefore that the charge profile of the same physical object in the XZ and YZ projection should be very similar.

Let's assume we have in the XZ projection a vertex v_X, with associated tracks tr_1^X and tr_2^X, and in the YZ projection a vertex v_Y, with associated tracks tr_1^Y and tr_2^Y. Each vertex in the XZ (YZ) projection has a position (X_v, Z_v^x) $((Y_v, Z_v^Y))$. Each track in the XZ (YZ) projection has a direction $(u^X, 1)$ $((u^Y, 1))$. First we require that the Z coordinate of v_X and v_Y are close ($|Z_v^X - Z_v^Y| < 10$mm. Then we measure the correlation factor of the charge profiles for each pair of tracks (tr_i^X,tr_j^Y). If, for example, (tr_1^X,tr_2^Y) is the pair with maximum correlation factor, we get a 3D vertex with the following parameters:

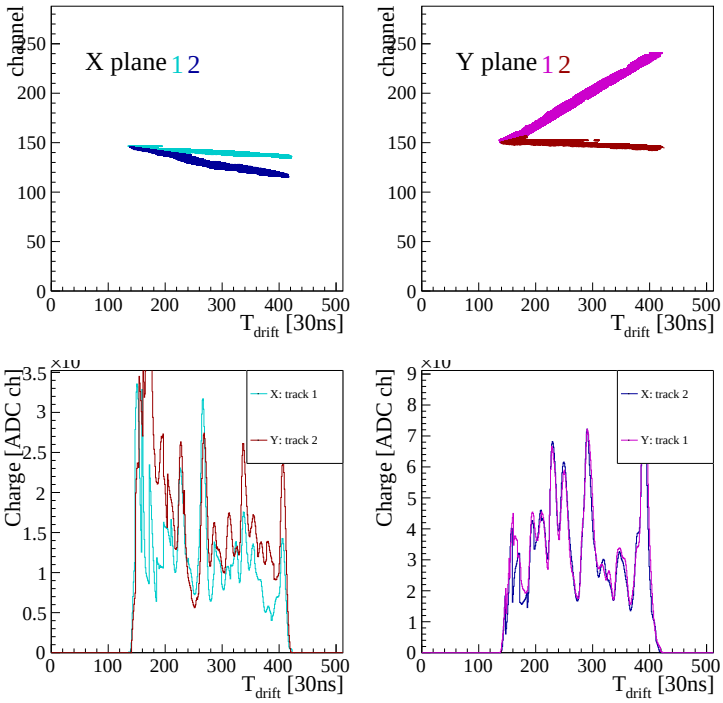

Figure 6: Procedure for matching the two projections of a vertex. Top: definition of the region associated to each of the two particles in the vertex. Middle: comparison of the charge profile (in Z direction) of X-Y track combinations. The covariance of these distributions is used to select the best match.

- Position: $\vec{X_v} = (X_v, Y_v, (Z_v^Y + Z_v^Y)/2))$
- Track A: direction $\vec{u_A} = (u_1^X, u_2^Y, 1)$
- Track B: direction $\vec{u_B} = (u_2^X, u_1^Y, 1)$.

We have no way of knowing which of the two track (A or B) corresponds to the electron or the positron, but this does not affect any of our measurements.

5 Results on polarimetry

We use the vertex information to study the resolution and polarimetry potential of the detector. A first measurement of this observable was already obtained with a previous version of the event reconstruction (version 2.0). That version had a much lower efficiency, and the preliminary results were presented and published [23].

5.1 Reconstruction efficiency

As explained above, there is, for now, no procedure for selecting vertices based on the event characteristics. Instead, we use here the fact that we know exactly the source of the photons. We select therefore the vertices located within the photon beam (which is clearly localised [24]). The following results are obtained using all of the reconstructed vertices in the data, applying only a space cut around the photon beam.

The work in [24] has shown that the trigger efficiency of the HARPO experiment was above 50% for all configurations. For this it identified detection events using the first signal in the TPC. If this signal is located within the beam region, the event is assumed to be an interaction of the beam with the gas. Using this definition, we can define the reconstruction efficiency as the fraction of those where a vertex is reconstructed and passes the cut mentioned above.

We find that the reconstruction efficiency is close to 90% in the configurations we used. These results are consistent with the simulation.

5.2 Polarimetry

We define the azimuthal angle ω_{+-} of the conversion into an e^+e^- pair of a photon propagating along the Z direction (see Fig. 3 in [7]):

$$\omega_{+-} = \arctan\left(u^Z_{e^+}u^X_{e^-} - u^Z_{e^+}u^X_{e^-}, u^Z_{e^+}u^Y_{e^-} - u^Z_{e^+}u^Y_{e^-}\right) \tag{2}$$

The cross-section σ_{conv} of conversion for a photon beam with a linear polarisation fraction P is:

$$\sigma_{conv} \propto 1 + A_{QED}P\cos(2\omega_{+-}) \tag{3}$$

where A_{QED} is the polarisation asymmetry of the conversion process.

Therefore the distribution of the measured azimuthal angle ω, defined as:

$$\omega = \arctan\left(u^Z_A u^X_B - u^Z_A u^X_B, u^Z_A u^Y_B - u^Z_A u^Y_B\right) \tag{4}$$

will follow a distribution:

$$1 + A_{eff}P\cos(2\omega_{+-}) \tag{5}$$

where $A_{eff} < A_{QED}$ is the effective polarisation asymmetry, taking into account the finite resolution of the detector. The measured distribution of ω for 11.8 MeVphotons is shown in Fig. 7 (top).

We see that there are large systematic fluctuations, mostly related to the cubic geometry of the detector. The resulting ω distribution with an unpolarised beam is shown in Fig. 7 (middle). By taking the ratio of these two distributions, we cancel all of the systematic fluctuations related to the geometry. The result (Fig. 7, bottom) shows clearly the modulation due to the beam polarisation.

Finally, we combine the data from the 4 angular configurations of the HARPO detector around the beam axis. Figure 8 shows the resulting distribution. The cosine modulation is very clear, with an asymmetry parameter $A^{beam}_{eff} = 7.4 \pm 0.6\%$.

We apply the same analysis to simulated data. We simulate pair-conversion events with a conversion point within the beam region of the detector. No background is included in the simulation. Figure 9 shows the polarisation modulation obtained. We compare this with what would be obtained with ideal tracking (ignoring all detector effects). We use the exact same procedure, replacing the values of $\vec{u_A}$ and $\vec{u_B}$ by the Monte Carlo values. For 11.8 MeV photons, we find a theoretical asymmetry of $A_{QED} = 16.4 \pm 0.7\%$ [25], and an effective value of $A^{sim}_{eff} = 10.3 \pm 0.6\%$. The effective value is significantly higher than the $A^{beam}_{eff} = 7.4 \pm 0.6\%$ from the beam data.

5.3 Effects of the tracking resolution on the polarimetry

The finite tracking resolution of the detector degrades the effective asymmetry A_{eff}. Figure 10 shows the effective polarisation asymmetry variation with the tracking resolution. We can see that for each energy, there is a critical resolution where the asymmetry drops. At higher energies, the opening angle of the e^+e^- pair become smaller, so that the resolution

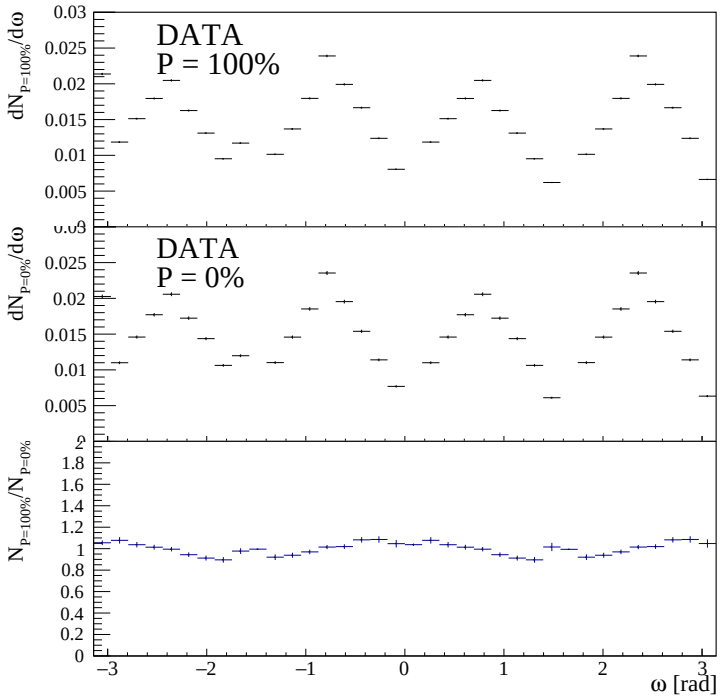

Figure 7: Distribution of the azimuthal angle ω for 11.8 MeVphotons in one angular orientation of the detector. Top: fully polarised photon beam. There are large systematic fluctuations. Middle: unpolarised photon beam. Bottom: ratio of the two above distributions. The systematic effects from the detector geometry cancel out, and the polarisation modulation appears clearly.

of the tracks has more effect on the azimuthal angle, and this critical resolution becomes smaller.

Using the Monte-Carlo information, we can find the track resolution σ_{track} (68 % containment) in the simulation. For 11.8 MeV photons, we find $\sigma_{track} = 8.79 \pm 0.19\,^\circ = 153 \pm 3$ mrad. We see in Fig. 10 that the expected corresponding asymmetry is $A_{eff} \approx 7.3\,\%$. This value is actually smaller than the one obtained after the full simulation and reconstruction. This shows that the approximation of Gaussian, non-correlated errors on the two tracks is excessive. In particular, since the two tracks are reconstructed simultaneously in the vertex, their resolution is necessarily correlated.

5.4 Systematic effects on the polarimetry

We see a significant difference between the measured asymmetry $A_{beam} = 7.4 \pm 0.6\%$ and the value obtained from simulation $A_{eff} = 10.6 \pm 0.8\%$. It is clear from Fig. 8 that the distribution is not exactly a cosine, with in particular peaks at $\pm\pi/2$. The method we used cancels all of the systematic effects related to the detector geometry and the reconstruction. The main remaining source of systematic errors is the beam itself.

There are two background contributions from the beam:

- Compton scattering of the photons. These can be misidentified as pair conversions due to the saturation effects. The Compton signal is also affected by polarisation.

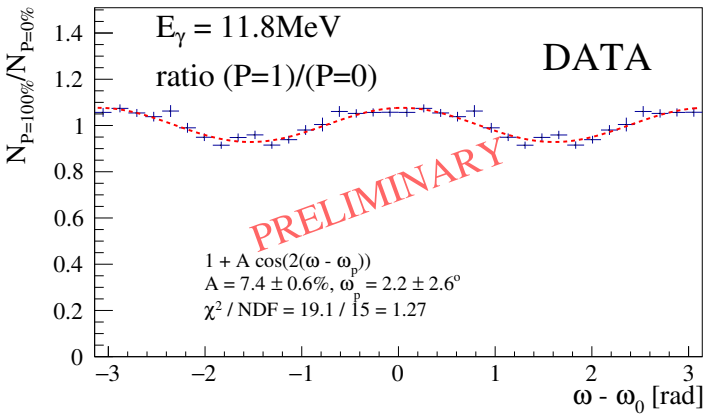

Figure 8: Polarisation modulation for a beam of 11.8 MeV photons. The plot is obtained by dividing data taken with a polarised beam and data taken with a non polarised one. Most of the systematic errors are cancelled, only statistical errors are shown.

- Bremsstrahlung from the electron beam. This gives an unpolarised contribution, with a wide energy distribution. The contribution of bremsstrahlung can vary between runs, due to the variability of the laser intensity, so that the related systematic effects may not completely cancel.

These effects have not yet been quantitatively studied.

The results featured in this article show only statistical errors. A future publication will give final results including systematic uncertainties.

6 Ongoing work and improvements

The results shown in these proceedings are still preliminary, using the version 3.0 of the reconstruction and analysis software of the HARPO experiment. There is ongoing work to improve these results, with in particular:

- Improvements on the vertex identification and selection.
- Improvements on the tracking to obtain a better angular resolution and momentum estimation from scattering.
- Understanding and quantification of the background contamination of the beam data.
- Calibration of the simulation, and addition of the background, in order to accurately estimate and correct the systematic fluctuations of the azimuthal angle modulation.

7 Conclusions and outlook

The HARPO detector was completed and used successfully in a photon beam in 2014. A full simulation of the detector was developed to describe it. A novel reconstruction algorithm was developed to cope with the unusual event topology.

Even before any optimisation was performed, these tools allowed us to measure the polarisation asymmetry of a 11.8 MeV photon beam with high precision, and with good

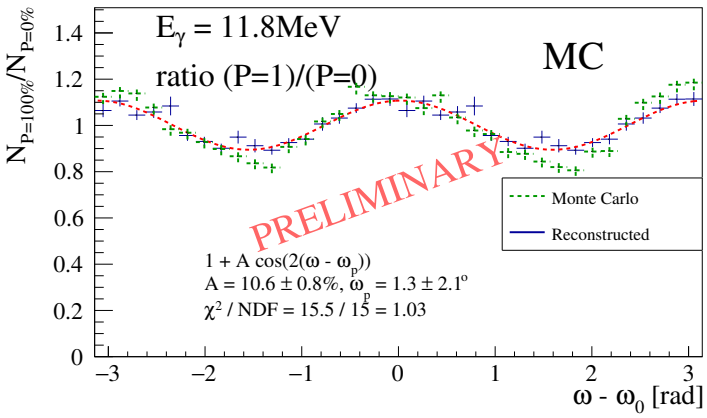

Figure 9: Polarisation modulation for a simulated beam of 11.8 MeV photons. The plot is obtained by dividing the data taken with a polarised beam by the data taken with a non polarised one. Most of the systematic errors are cancelled, only statistical errors are shown. In green, the same distribution is made using the exact (i.e. from Monte Carlo) electron and positron direction.

agreement with simulation. Some discrepancies remain, and will be addressed by the ongoing analysis and reconstruction developments.

The results from the beam data are extremely encouraging and studies are under way to adapt this technology for use as a space telescope.

ACKNOWLEDGMENTS

This work is funded by the French National Research Agency (ANR-13-BS05-0002) and was performed by using NewSUBARU-GACKO (Gamma Collaboration Hutch of Konan University).

References

[1] V. Schoenfelder, "Lessons learnt from COMPTEL for future telescopes," *New Astronomy Reviews*, vol. 48, pp. 193–198, 2004.

[2] M. Ackermann *et al.*, "The Fermi Large Area Telescope On Orbit: Event Classification, Instrument Response Functions, and Calibration," *Astrophys. J. Suppl.*, vol. 203, p. 4, 2012.

[3] M. Tavani, V. Tatischeff *et al.*, "The ASTROGAM gamma-ray space mission; A sensitive observatory for the MeV - GeV domain," In preparation.

[4] Xin Wu, Meng Su *et al.*, "PANGU: A High Resolution Gamma-ray Space Telescope," *Proc.SPIE Int.Soc.Opt.Eng.*, vol. 9144, p. 91440F, 2014.

[5] A. Moiseev *et al.*, "Compton-Pair Production Space Telescope (ComPair) for MeV Gamma-ray Astronomy," *ArXiv e-prints*, 2015.

[6] D. Bernard, "TPC in gamma-ray astronomy above pair-creation threshold," *Nucl. Instrum. Meth. A*, vol. 701, p. 225, 2013.

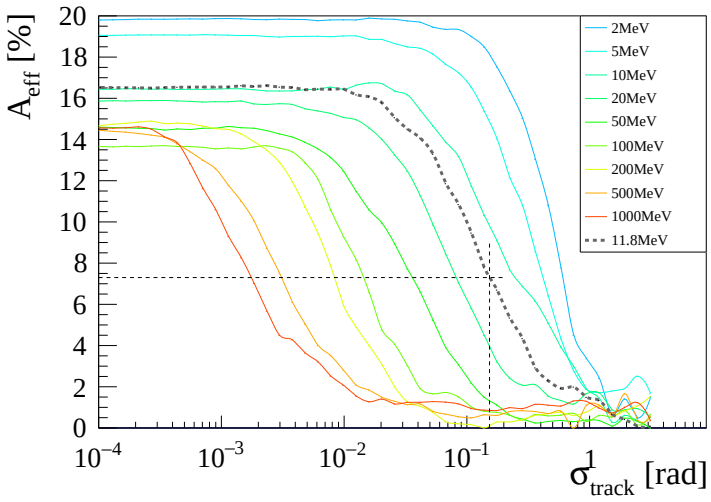

Figure 10: Effective polarisation asymmetry as a function of tracking resolution for different photon energies.

[7] D. Bernard, "Polarimetry of cosmic gamma-ray sources above e^+e^- pair creation threshold," *Nucl. Instrum. Meth. A*, vol. 729, p. 765, 2013.

[8] J. R. Mattox, "Analysis of the COS B data for evidence of linear polarization of VELA pulsar gamma rays," *Astrophysical Journal*, vol. 363, pp. 270–273, 1990.

[9] H. Zhang and M. Böttcher, "X-Ray and Gamma-Ray Polarization in Leptonic and Hadronic Jet Models of Blazars," *Astrophys. J.*, vol. 774, p. 18, 2013.

[10] P. Gros *et al.*, "HARPO - TPC for High Energy Astrophysics and Polarimetry from the MeV to the GeV," *Proceedings of Science*, vol. TIPP2014, p. 133, 2014.

[11] D. Calvet, "A Versatile Readout System for Small to Medium Scale Gaseous and Silicon Detectors," *IEEE Trans. Nucl. Sci.*, vol. 61, no. 1, pp. 675–682, 2014.

[12] K. Horikawa, S. Miyamoto, S. Amano, and T. Mochizuki, "Measurements for the energy and flux of laser Compton scattering γ-ray photons generated in an electron storage ring: NewSUBARU," *Nuclear Instruments and Methods in Physics Research Section A: Accelerators, Spectrometers, Detectors and Associated Equipment*, vol. 618, no. 1-3, pp. 209 – 215, 2010.

[13] S. Wang *et al.*, "HARPO: a TPC concept for γ-ray polarimetry with high angular resolution in the MeV-GeV range," *J. Phys. Conf. Ser.*, vol. 650, p. 012016, 2015.

[14] H. Hirayama, Y. Namito, A. F. Bielajew, S. J. Wilderman, and W. R. Nelson, "The EGS5 code system," 2005.

[15] F. Salvat, "The penelope code system. Specific features and recent improvements," *Annals Nucl. Energy*, vol. 82, pp. 98–109, 2015.

[16] J. Allison *et al.*, "Geant4 developments and applications," *IEEE Transactions on Nuclear Science*, vol. 53, pp. 270–278, Feb 2006.

[17] M. L. Iparraguirre and G. O. Depaola, "Pair production by gamma-rays on electrons. Threshold for the momentum recoil detection," *Eur. Phys. J.*, vol. C71, p. 1778, 2011.

[18] P. Christiansen, A. Dobrin, P. Gros, H.-Å. Gustafsson, M. Ivanov, M. Kowalski, A. Oskarsson, L. Österman, and E. Stenlund, "The influence of detector effects on TPC performance ," *Nuclear Instruments and Methods in Physics Research Section A: Accelerators, Spectrometers, Detectors and Associated Equipment*, vol. 609, no. 23, pp. 149 – 155, 2009.

[19] P. Christiansen, P. Gros, L. Jönsson, M. Ljunggren, B. Lundberg, U. Mjörnmark, A. Oskarsson, E. Stenlund, L. Österman, K. Fujii, and R. Yonamine, "Particle tracking and energy loss measurements with the LCTPC: A comparison to simulation models." http://www.eudet.org/e26/e28/, 2010. "EUDET-Memo-2010-36".

[20] S. Biagi, "Monte carlo simulation of electron drift and diffusion in counting gases under the influence of electric and magnetic fields," *Nuclear Instruments and Methods in Physics Research Section A: Accelerators, Spectrometers, Detectors and Associated Equipment*, vol. 421, no. 12, pp. 234 – 240, 1999.

[21] R. O. Duda and P. E. Hart, "Use of the Hough Transformation to Detect Lines and Curves in Pictures," *Commun. ACM*, vol. 15, pp. 11–15, Jan. 1972.

[22] R. Fruhwirth, "Application of Kalman filtering to track and vertex fitting," *Nucl. Instrum. Meth.*, vol. A262, pp. 444–450, 1987.

[23] Y. Geerebaert, P. Gros, S. Amano, D. Attié, D. Bernard, P. Bruel, D. Calvet, P. Colas, S. Daté, A. Delbart, M. Frotin, B. Giebels, D. Götz, S. Hashimoto, D. Horan, T. Kotaka, M. Louzir, Y. Minamiyama, S. Miyamoto, H. Ohkuma, P. Poilleux, I. Semeniouk, P. Sizun, A. Takemoto, M. Yamaguchi, and S. Wang, "Measurement of 1.7-74 MeV polarised rays with the HARPO TPC ," *Nuclear Instruments and Methods in Physics Research Section A: Accelerators, Spectrometers, Detectors and Associated Equipment*, pp. –, 2016.

[24] S. Wang, *Étude d'une TPC, cible active pour la polarimétrie et l'astronomie gamma par création de paire dans HARPO*. PhD thesis, École Polytechnique, 9 2015. in French.

[25] Y. D. Kotov, "Methods of measurement of gamma-ray polarization," *Space Science Reviews*, vol. 49, p. 185, 1988.